Journal of Molecular Liquids 315 (2020) 113700

Contents lists available at ScienceDirect

Journal of Molecular Liquids

journal homepage: www.elsevier.com/locate/molliq

Direct insights into the micro and macro scale mechanisms of symbiotic effect of SO_4^{2-}, Mg^{2+}, and Ca^{2+} ions concentration for smart waterflooding in the carbonated coated micromodel system

A. Maghsoudian [a], A. Esfandiarian [a], S. Kord [a,*], Y. Tamsilian [b,*], B. Soltani Soulgani [a]

[a] Department of Petroleum Engineering, Ahvaz Faculty of Petroleum, Petroleum University of Technology, Ahvaz, Iran
[b] Department of Chemical Engineering, Faculty of Engineering, Shahid Chamran University of Ahvaz, Ahvaz, Iran

ARTICLE INFO

Article history:
Received 11 April 2020
Received in revised form 24 June 2020
Accepted 26 June 2020
Available online 27 June 2020

Keywords:
Smart water
Pore-scale mechanism
Carbonated coated micromodel
Wettability alteration
Oil recovery

ABSTRACT

Up to now, a large number of studies revealed that smart waterflooding is a cost-effective method by considering the effect of potential determining ions (PDI) on enhanced oil recovery (EOR) in the carbonated reservoir. Current research studied the symbiotic effect of different ions concentration (SO_4^{2-}, Mg^{2+}, and Ca^{2+}) template in smart water with a constant salinity (40,572 ppm) to justify effective mechanisms at macro and micro scale in a coated carbonated micromodel system. A set of experimental tests such as X-ray diffraction (XRD), compatibility, zeta potential, interfacial tension (IFT), and contact angle (CA) were conducted to determine the type of rock and examine the effect of ions on oil/brines/rock interaction, combined with carbonated coated micromodel flooding tests to determine the optimum smart water solution. Zeta potential tests revealed that the excess amount of SO_4^{2-} and Mg^{2+} changed the surface charge into highly negative and positive ones, respectively. Two times excess amount of SO_4^{2-} (SW2S) had a key role to alter the wettability by measuring CA from 40° to 147°, however, no considerable relation among oil/brines interaction was observed for the IFT reduction. Findings corroborated that Ca^{2+} and SO_4^{2-} were the major components for desorbing the carboxylic group from the calcite surface at room temperature. The carbonated coated micromodel flooding results showed that SW2S led to higher ultimate oil recovery (~38%), reconfirmed that wettability alteration was the main mechanism and resulted in better pore-scale performance by less amount of residual oils and discontinuities around the carbonated coated grains.

1. Introduction

Importance of the enhancements in the oil recovery has been increased because of limited numbers of the oil reservoirs. As a fact, the recovery factors of sandstone reservoirs are dominant than carbonates due to the presence of harsh conditions in the carbonated reservoir [1,2]. Therefore, finding an appropriate method to augment enhanced oil recovery (EOR) is one of the most vital steps in the oilfield development plans, especially in the carbonated reservoir. Smart waterflooding has become one of the most essential EOR processes due to their potential benefits in the oil recovery enhancement compared to the conventional sea water (SW) injection [1]. Adjusting/optimizing of different types of salts by changing in their concentration which resulted in altering the initial equilibrium of porous media is well-known as smart water and it can be applied in secondary and tertiary recovery process [3,4]. It has a great potential to effect on the rock/fluid and fluid/fluid mechanisms in oil reservoirs toward the more water-wet condition and optimize the ultimate oil recovery in the porous medium [5–7]. Changing the waterflood salinity/chemistry can increase oil recovery from carbonate reservoirs by 5–25%; however, the main mechanisms that participated in this method are still unclear [6,8–10].

A large number of hypotheses and mechanisms have been recommended to explain the effect of the smart water injection on the oil production, including the increase in pH to in-situ saponification, change the surface charge, and decrease the interfacial tension (IFT) [11–14], fines migration [15,16], multicomponent ionic exchange (MIE) [17,18], double-layer expansion (DLE) [19–21], and wettability alteration [22–25]. The present literatures proposed the wettability alteration as the most effective mechanism [2,6,26], however, side effects mechanisms such as surface ion exchange, surface charge change, and DLE considerably impacted at the pore-scale [2,27,28]. Studying on the wettability alteration mechanisms based on the effect of existing ions in the aqueous solution was initiated in the 2000s which became the cornerstone for the further development by researchers [2,22,29]. For the first time in 2005, Hoegnesen et al. investigated the impact of changes in the ionic composition of the carbonate reservoir resulting from the smart water

* Corresponding authors.
E-mail addresses: sh.kord@put.ac.ir, soltani.b@put.ac.ir (S. Kord), tamsilian@scu.ac.ir (Y. Tamsilian).

https://doi.org/10.1016/j.molliq.2020.113700
0167-7322/

injection. In this study, researchers used sea water with 33,000 ppm concentration as a base fluid where the concentration of SO_4^{2-} ion was changed as a potential determining ion (PDI) at various temperatures (70–130 °C). They observed that spontaneous imbibition rate increased at higher levels of temperature and SO_4^{2-} concentration [30]. In the following, a large number of studies were carried out on symbiotic and individual impacts of various divalent ions on proposed mechanisms such as wettability alteration by measuring fluid-solid contact angle (CA) [5,7,17,23,26,31–33], IFT reduction [25,34–36], DLE [21,37–39], rock dissolution [5,37,40,41], and change the surface charge (zeta potential) [14,26,42] in carbonated rocks at both room and high temperature. Findings illustrated that there were several mechanisms participated in smart waterflooding in carbonated reservoirs; although the wettability modification into water-wet state for the ultimate oil recovery could be the main cause during smart water injection. However, this alteration and related mechanisms is still unclear and needs more discussions.

Up to now, in experimental scale most researches have been focused on the core scale by conducting core flooding and spontaneous imbibition experiments [2,6,25,27,43–46] and there is no investigation of the smart water effects through the pore-scale like the glass micromodel visualization. Other side, most of the pore-scale micromodel investigations have been implemented for the sandstone reservoirs under a range of temperature and salinity because of micromodel characteristics mainly similar to the sandstone [1,47–51]. Ding et al. in 2019, a series micro and macroscopic experiments implemented in chalk rock by applying μ-CT images. Results demonstrated that decreasing the Ca^{2+} concentration was more effective than excess amount of SO_4^{2-} in the wettability alteration state into water-wet [52]. In 2020, Mohammadi and Mahani conducted a visually test on the etched carbonated micromodel (Spar calcite) to evaluate the impact of low salinity waterflooding (LSW) after the high salinity water injection. Their results visually showed that LSW had a great potential to increase the ultimate oil recovery by considering wettability alteration mechanism in the micromodel [53].

Current researches evidently imply that low salinity/smart waterflooding can lead to the additional oil recovery. Therefore, two salient features, the cost-effectiveness and easy accessibility, would make this process a promising candidate for an enhanced oil recovery. Although, carbonated rocks still suffer from lack of sufficient mechanistic analyses at pore-scale and rock complexities. Furthermore, the uptake of underlying chemical and physical interaction in individual and symbiotic effect of ions to better understanding mechanisms requires more specific investigation to determine the most effective and appropriate smart water solution. In this paper, the influence of symbiotic behavior of different ions concentration (SO_4^{2-}, Mg^{2+}, and Ca^{2+}) on the compatibility, surface charge, wettability alteration, and IFT reduction was investigated. For the first time, the carbonated coated glass micromodel was applied to investigate about the underlying pore-scale mechanisms of smart water solutions in a carbonated reservoir. The outcomes of this research would be lucrative to determine an appropriate concentration of divalent ions during the smart waterflooding in the coated carbonated micromodel at both micro and macroscopic scale. Herein, firstly, the determination of oil properties and brines' calculation were performed. Next, the smart water preparation, micromodel manufacturing, and XRD test were conducted. Finally, a set of experimental tests including compatibility, IFT, zeta potential (pure calcite and smart water solutions), and CA experiments alongside the flooding experiments in a carbonate coated micromodel were carried out to determine the optimum smart water solution.

2. Materials and methodology

2.1. Materials

Six different kinds of salts dissolved in deionized water including NaCl, KCl, $CaCl_2$, $MgCl_2(6H_2O)$, Na_2SO_4 and $NaHCO_3$ provided by the Merck Company (Germany) with 99% purity were used to prepare synthetic smart water solutions. Synthetic sea water was prepared based on the Persian Gulf sea water components and the total dissolved salinity (TDS) of 40,572 ppm. Nine types of smart waters were synthesized with the same TDS of SW. For instance; double concentration of Mg^{2+} denoted by the symbol of SW2Mg in the smart water was compared to the SW at the constant concentrations of Ca^{2+} and SO_4^{2-}. Specification of all brines used in this study are given in Table 1. The order of adding salt into DIW was so important since it could increase the final stability up to 10 times higher than the other methods. Therefore, the process started with divalent cation brine ($CaCl_2$ and $MgCl_2.6H_2O$), and sequentially continued by adding NaCl, KCl, Na_2SO_4, and $NaHCO_3$ [23]. Moreover, formation brine (FB), a slight amount of Sr^{2+} (1460 ppm), NO_3^- (153 ppm), and Li (5 ppm) included, was used to carried out the compatibility tests, the composition is listed in Table 2.

The crude oil sample was prepared from one of the southern Iranian oilfields. The polarity of the crude oil referred to the heteroatoms such as sulfur, nitrogen, and oxygen existing in the functional groups of acidic and basic organic molecules in the crude oil such as the asphaltene and resins. Using a filtration paper with an average pore diameter of 5 mm in addition to a vacuum pump allowed the solid particle to be removed from the sample. The chemical specification analysis of the sample is listed in Table 2. Viscosity, density, and asphaltene content were measured using Cannon Fenske viscometer (size = 200, Cannon Instrument Company, USA), DMA45 digital densitometer (Anton Paar, Austria), and modified method of standard IP143 method [54], respectively.

2.2. Methodology

The micromodel patterns and characteristics presented in Fig. 1a, b and Table 3 including single fracture, and double permeability solid matrix, was designed to examine the impact of the smart waterflooding in a porous medium. The micromodel developed in this study consisted of two glass plates with 6 mm thickness, 140 mm in length, and 60 mm in width designed by well-known and high technology software.

The micromodel setup included a camera (EOS 70D, Canon, Japan) to capture high-quality pictures, a precise differential pressure to measure the pressure for the absolute permeability determination, a high accuracy syringe pump (SP102 HSM, Fanavaran Nano-Meghyas, Iran) to control the fluids flow through the micromodel medium, and a light source for a better insight at the pore scale. After each flooding test, the glass micromodel was cleaned by the toluene, next by acetone and distilled water flush and finally became post-flushed by HCl acid to revert the glass micromodel into the initial condition (water-wet) [55–57]. To consider the actual operation in the field consisting capillary number, turbulent flow, and feasibility in the experimental study, the importance of the viscous forces referring to capillary forces was characterized using the classical macroscopic capillary number, $N_{Ca} = \eta_{water} \times v_{inj} / \gamma$, where $\gamma = 22.1\ dyne/cm$ showing the interfacial tension between the crude oil and deionized water, and $\eta_{water} = 1\ mPa{\cdot}s$ and $v_{inj} = Q/bd$, $Q\ (mL/h)$ is the injection rete for displacing phase, b and d are the characteristic injection velocity for an average depth b (μm) and a pore-throat size d (μm), respectively. The injection rate of the displacing phase would be optimum to be in the specific range of capillary number which is 10^{-4} to 10^{-6} for carbonated reservoirs [58]. Since the flow regime thought the porous media and in the middle of the reservoir was laminar, the injection rate (Q) and the capillary number were selected as 0.05 mL/h and 3×10^{-5}, respectively. During the entire injection tests, the flow was set at a constant rate and the micromodel was placed horizontally under the ambient conditions. All the flooding processes were performed as the secondary flooding and without the pre-flush. The flooding process stopped after 2 pore volume (PV) injections where the operation time was approximately 32 h. In the presence fracture, the aqueous solutions phase displaced automatically oriented to move into the direction of the fracture route due to the zero-capillary pressure. Hence, the displacing fluid depleted the wetting

Table 1
Brine composition in synthetic smart water.

Brines	Na^+ (ppm)	K^+ (ppm)	Cl^- (ppm)	Mg^{2+} (ppm)	Ca^{2+} (ppm)	SO_4^{2-} (ppm)	HCO_3^- (ppm)	Concentration (ppm)	pH	Ionic strength (mmol/l)	Density (g/mL)
FB	72,698	303	115,375	585	5950	168	396.50	195,475 + 1618	7.3	6446	1.1106
SW	12,290	280	22,652	1530	460	3210	122	40,572	8	1291	1.0053
SW0Mg	14,893	280	21,579	0	460	3210	150	40,572	7.96	1311	0.9960
SW0Ca	13,037	280	22,365	1530	0	3210	150	40,572	8.01	1304	1.0018
SW0S	12,867	280	25,285	1530	460	0	150	40,572	7.75	1357	0.9953
SW2Mg	10,179	280	23,233	3060	460	3210	150	40,572	7.56	1278	1.0006
SW2Ca	12,035	280	22,447	1530	960	3210	150	40,572	7.92	1286	1.0059
SW2S	12,205	280	19,527	1530	460	6420	150	40,572	7.96	1233	0.9986
SW4Mg	5464	280	24,888	6120	460	3210	150	40,572	7.14	1246	0.9966
SW4Ca	11,033	280	22,529	1530	1840	3210	150	40,572	7.35	1267	0.9946
SW4S	11,544	280	13,768	1530	460	12,840	150	40,572	8.09	1108	0.9979

phase in the channel completely, then the fluid started to transfer from the fracture to the matrix led to better displacement procedures between the two matrices. To calculate the ultimate recovery factor during the displacement procedure, the image processing technique was implemented. A dinolite camera (AM-413ZT model, 200×, 1.3 M pixel, Taiwan) was used to investigate about the pore-scale phenomena and mechanisms.

The glass micromodel was made of 90% silica (SiO_2), where its mineralogy was very similar to the properties of sandstone rock. Coating with carbonated powders was applied as a new approach to alter the porous media properties and make it analogous to the carbonated surface. In this regard, the first step was to prepare a suspension of calcium carbonated powder suitable for the injection, avoiding critical deposits in the glass micromodel. An injection process had to be contrived for the actual powder coating of the pore network, requiring several tests before establishing an optimized and successful protocol. Finally, the suitable concentration of the dilute suspension of $CaCO_3$ powder was found as 2 wt% which resulted in avoiding the pore plugging and obtaining a homogeneous powder distribution in the pore network. In the following, the suspension injected into the glass micromodel by a general syringe at a high injection rate to postpone the powder precipitation. As a final step, drying procedure performed in the oven at 100 °C for five days where the selected temperature did not let any clay degradation [59]. Moreover, carbonate powder settled in the micromodel space inside the pores and on the glass surface. Powder distribution was almost constant during injection due to very low flowrate (0.05 mL/h) and low viscosity of the injection phase. The results obtained after the coating procedure are displayed in Fig. 1c.

To make the carbonate coated micromodel into oil-wet medium, it was saturated with the crude oil for 48 h before each test. Fig. 1d, e, and f show how the micromodel and coated grain became oil-wet after 48 h aging with crude oil. In this study, contact angle method was used to show the change in the properties of the micromodel surface. The low-thickness calcite powder was pressed onto the glass surface to provide a very smooth and uniform layer. It was then placed in a furnace to keep the powder on the glass surface. Fig. 1g, h, and i demonstrates carbonated coated micromodel before and after aging with crude oil and after 168 h aging with SW2S as an appropriate smart water solution, respectively. Moreover, Fig. 1j, k, and l shows carbonated coated micromodel snapshot from surface roughness before and after aging and after aging with SW2S, respectively. Results illustrated the layer of carbonated powder precipitate changed the properties of the original quartz minerals. During each experiment, images were captured from the micromodel using a high-resolution camera (AM-413ZT model, 200×, 1.3 M pixel, Taiwan).

To minimize the uncertainty of glass micromodel and pore network properties determination, carbonated core samples were provided from one of the Iranian south oilfields to conduct the wettability alteration experiments. Core sample was given in the cylindrical form with 9 cm length and 2 cm in diameter. To prepare the thin slices for CA test, a core trimming machine was employed to cut the core samples into the horizontal slices. Soxhlet extraction was also used for the cleaning process by toluene to extract the hydrocarbon and later methanol to remove the salts. Then, all cleaned core samples were dried in an oven (~ 80 °C, 7 days). The slices were shaved and polished to reach a flat smooth surface which were aged in the same oil sample at 80 °C for 4 weeks to reach the oil-wet condition. The diameter and thickness of the rock slices were almost 1 cm and 3 mm, respectively. D8 Bruker X-ray diffraction (XRD) (Germany) device was used to determine the rock type of carbonated slices.

2.3. Measurements

2.3.1. Compatibility test

Various types of cations and anions ions in the smart water solutions may result in undesirable precipitation. Hence, two different types of compatibility experiments were carried out for the smart water solutions. The first experiment was implemented for all smart water solutions at high temperature (80 °C) to check the ions precipitation. For this purpose, 10 mL of smart water solutions were poured in the sealed tube tests and kept them in oven for one month. The second one focused on the behavior of smart water solutions in the presence of FB at high temperature (80 °C) after one month. In the following, 5 mL of smart water and 5 mL FB added to sealed tube and put them on the oven.

2.3.2. Zeta potential test

Calcite slice was crushed into fine powders and then soaked by deionized water in sealed bottle to determine point of zero charge (PZC). As well as, different pH values were adjusted by adding NaOH and HCl for above and under 7, respectively [2]. In the following, the sample

Table 2
Crude oil properties.

Properties	Density [g/mL]	API	Acid number [mg KOH/g oil]	SARA [wt%]				Viscosity [mPa·s]
				Saturates	Aromatics	Resins	Asphaltene	
Value	0.87	33	2.9	49.2	37.6	8.1	4.63	40.28

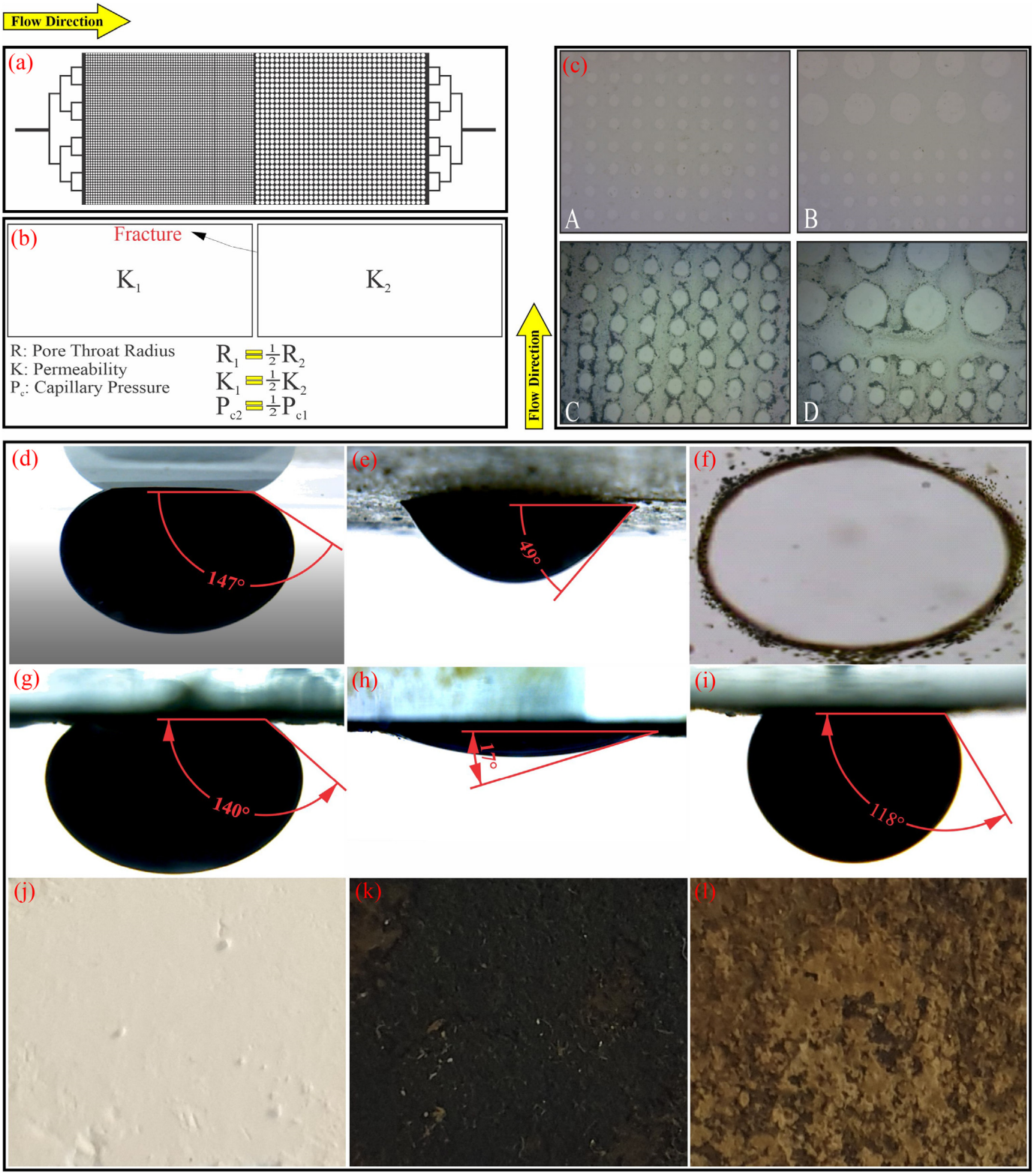

Fig. 1. a) Glass micromodel pattern, b) micromodel main characteristics, c) microscopic images of carbonated powder coating in glass micromodel (A and B before coating, C and D after coating), d) glass micromodel snapshot before aging and e) glass micromodel snapshot after 48 h aging with oil, f) surface coated grain still completely oil-wet after 32 h water injection, g) carbonated coated micromodel snapshot before aging, h) carbonated coated micromodel snapshot after 48 h aging with oil and i) carbonated coated micromodel snapshot after 168 h aging with SW2S, j) carbonated coated micromodel snapshot from surface roughness before aging, k) carbonated coated micromodel snapshot from surface roughness after aging, and l) carbonated coated micromodel snapshot from surface roughness after 168 h aging with SW2S.

Table 3
Glass micromodel specification.

Parameters	Value	Unit
Pore volume	0.787	cm^3
Porosity	53	%
Permeability	549	MD
Average depth	160	μm
Length	140	mm
Width	60	mm
Pore throat in high permeable zone	200	μm
Pore throat in low permeable zone	100	μm
Fracture length	60	mm
Fracture width	600	μm

was smoothly stirred for 48 h, after which the mixture was filtered by applying 0.45 μm filter papers under a vacuum pump. In the case of zeta potential experiment of smart water solutions, the crushed powders were applied for a solid/liquid solution by combining 0.125 g of the calcite powder to 20 mL of smart water solutions in a 25 mL sealed bottle [60]. The sealed bottle was put on a multi-wrist shaker for conditioning in ambient condition for 72 h. The conditioned suspensions were allowed to settle at room temperature for a minimum of 1 h until a clear suspension was visually seen through the tube. Then, the fine particles suspended in mixture were drained by a spinal needle and filtered with a 5 μm syringe filter to provide final sample and transferred into a standard cuvette for zeta potential tests. All zeta potential experiments were carried out at room temperature by applying a Micromertrics zeta potential analyzer (HORIBA, Japan). Each sample measurement was repeated 3 times to determine the mean value with ±4% standard error deviation bar.

2.3.3. Contact angle test

The contact angle method was used for the evaluation of the wettability alteration mechanism and checking the interaction of different fluids with rock slices, affecting capillary pressure, relative permeability, waterflooding behavior, and electrical properties [61]. After preparing the rock slices, all were immersed in oil for 40 days at 60 °C temperature while being kept in the oven. The effects of different brines on the wettability alteration were assessed using the sessile drop method under a simple and accurate setup in the ambient condition capturing the image of drop shape by a Dino-Lite Edge digital microscope (AM-413ZT model, 200×, 1.3 M pixel, Taiwan). A specific cross section was allocated for each contact angle test. Contact angle was recorded in 5 steps, initial condition (0 h), 24, 48, 72, and 168 h after aging with aqueous solutions. To generate trustworthy data, the angle recording time interval was set 15 min for all tests. Each CA test was repeated three times to report the mean value. Moreover, the contact angle values were reported from the inside of the oil droplets.

2.3.4. Interfacial tension test

The IFT value was calculated using the accurate image processing software. The rising bubble pendant drop method was also applied to measure the IFT value between different types of smart water and crude oil. The VIT 6000 apparatus (Fars Enhanced Oil Recovery Company, Iran) was carried out for IFT measurements at room temperature. Each IFT test was repeated four times to assess the stability of IFT values for different types of smart water and the mean IFT value was reported with the error bar deviation.

3. Results and discussion

3.1. Compatibility analysis

By visual analysis, it was clear that all of the ions were compatible in the aqueous solution and no significant precipitation was observed at 80 °C after one month, presented in Fig. 2a. These results confirmed that the priority of adding salts was an appropriate procedure which was completely eliminated the salt precipitation problem during the smart waters preparation.

Fig. 2b shows smart water solutions combined with FB at 80 °C. No precipitation was observed in the lower concentration of divalent cations and anion. Besides, the amount of precipitated solid material for SW4Mg and SW4Ca was negligible in the presence of formation brine. However, in the case of SW4S, the precipitation value was considerable compared to the other types of smart water. Findings illustrated that the optimum concentration for SO_4^{2-} was more essential than enhancing the concentration which could be control reservoir scaling during smart water flooding [62], especially in the presence of formation brine.

3.2. Wettability alteration measurement

Fig. 3 provides the results of the quantitative analysis with XRD and zeta potential performed on the powdered sample. Since there was only one sharp peak inside Fig. 3a, it could be concluded that the prepared sample had no impurities and the rock sample consisted of only one element (calcite, about 99%). The negatively charged acidic components of the crude oil were usually adsorbed onto the positively charged basic carbonate surface to create the Ca^{2+}-carboxylate complex on the rock surface where the wettability alteration occurred toward the more oil-wetness regions [12,63]. Results from zeta potential experiments demonstrated charge properties of calcite particles and suggested which ions from smart water solutions had more positive impact on adsorb and substitute charge according to pH values. Based on the results from Fig. 3b, PZC for the calcite powder was around pH~8.9 [40,64]. Besides, all pH smart water solutions were approximately between 7 and 8.1 (Table 1).

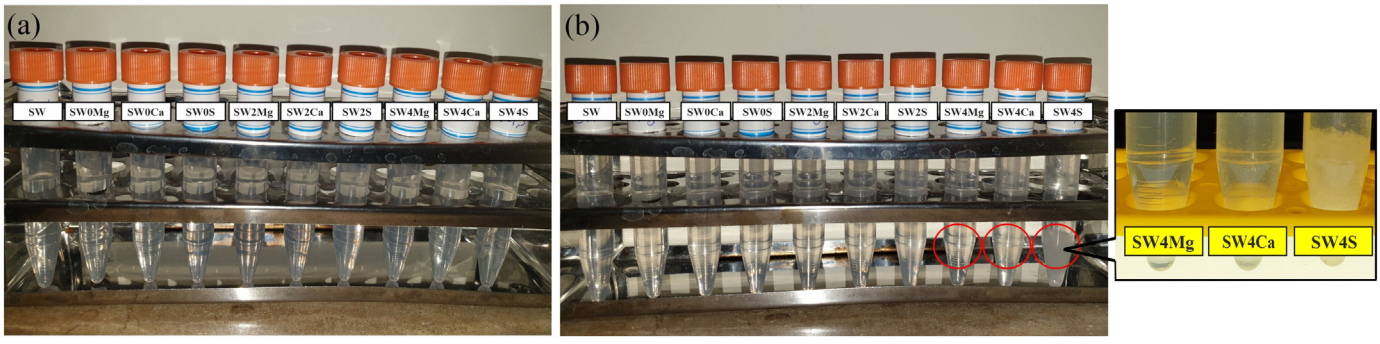

Fig. 2. Compatibility test for a) smart water solutions after two months in ambient condition and b) four times excess divalent ions in sea water combined with formation brine at high temperature (80 °C).

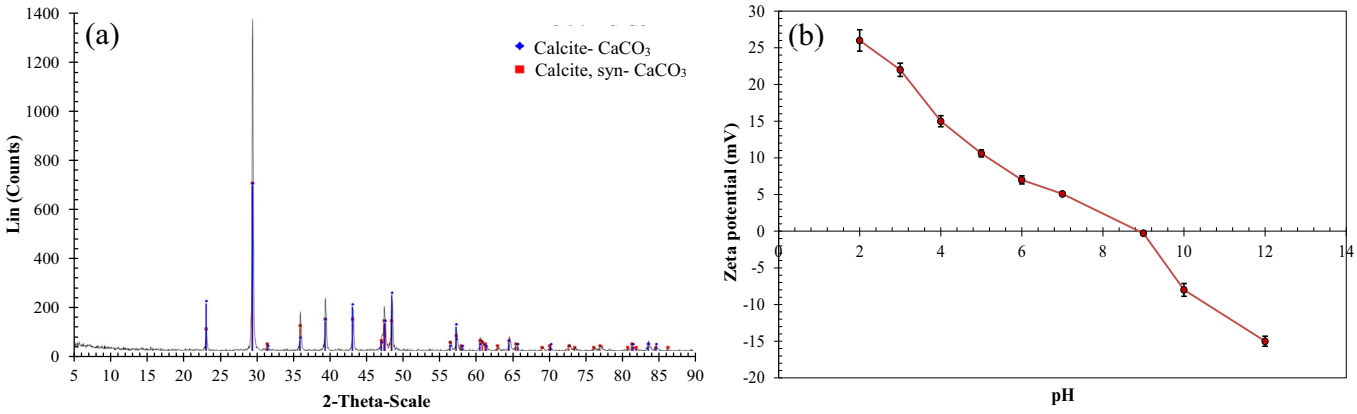

Fig. 3. a) XRD pattern of calcite sample from an Iranian carbonate reservoir and b) zeta potential of pure calcite fine particles in deionized water at room temperature.

3.2.1. Effect of divalent cations on zeta potential

Fig. 4 illustrates the zeta potential of high purity calcite powder in the presence of different brines solution. SW had a negative charge (−6.35 mV) related to the ratio of divalent anion and cations concentration. The SO_4^{2-} concentration was 2 times higher than Mg^{2+} and 6 times higher than Ca^{2+} in SW (3210, 1530, 460 ppm, Table 1), confirming the negative value of SW on the calcite surface charge.

The calcite powder was aged in 10 different types of smart water solution. Adding calcite powder in solutions form a stern layer of adsorbed ions while the hydrated ions stayed in solution. Therefore, different ions concentrations in aqueous solutions created a various double layer expansion area, led to modify calcite surface charge based on the different amounts of divalent and monovalent ions. According to results from Fig. 4, the highest zeta potential values were related to excess amount of divalent cations of SW4Mg (8.18 mV), SW4Ca (5.04 mV), and SW2Mg (4.36 mV), respectively. Increasing the concentration of Mg^{2+} had a significant effect on changing the surface charge from negative to highly positive, presenting a linear ascending relation between zeta potential value and Mg^{2+} concentration. Both Mg^{2+} and Ca^{2+} were known as alkaline earth metal from the Mendeleev's periodic table. Therefore, Mg^{2+} had a weak base behavior and while a hydration bond break and change into H^+ and OH^-, Mg^{2+} tend to interact with OH^- (due to high concentration) making more the acidic environment and pH decreased (Table 1). Furthermore, the same process was true for Ca^{2+}, however, the rate of pH change was lower compared to Mg^{2+} due to lower concentration and atomic number [65]. In case of SW2Ca, the sum of divalent cations was lower than sum of divalent anions (920 + 1530 < 3210 ppm) resulted in the higher pH (7.92) and negative surface charge (−2.87 mV) compared to four times excess Ca^{2+}. In other side, SW4Ca had a great impact on altering the surface charge and made it positive (1530 + 1840 > 3210 ppm) and lowering pH number (7.35). Based on the ratio of divalent cations and anion and pH value, results demonstrated a considerable effect of Mg^{2+} ions concentration on the behavior of SO_4^{2-} ions to alter the original surface charges of calcite into positive, while the excess amount of Ca^{2+} ions had lower effect compared to Mg^{2+} on modifying the surface charge in the presence SO_4^{2-}, especially in 2 times excess amount of Ca^{2+} [12,60].

3.2.2. Effect of divalent anion on zeta potential

Based on the results for SW4S, a linear descending relation was observed among the excess amount of SO_4^{2-} and surface charge. SO_4^{2-} having a strong acidic property interacted with H^+ while hydration bond breakdown to create more basic environment and increase pH (Table 1). In two- and four-times excess amount of SO_4^{2-}, the negatively charge slightly and strongly increased compared to SW respectively

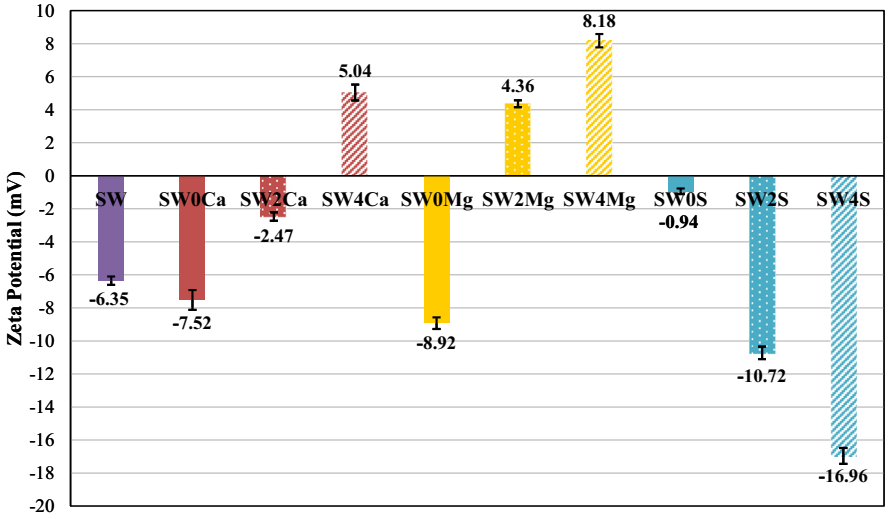

Fig. 4. Zeta potential of calcite fine particles aged in various brines including sea water (SW), and different divalent ions concentrations (Ca^{2+}, Mg^{2+} and SO_4^{2-}) at room temperature.

(−10.72 and − 16.96 mV versus −6.35 mV). This behavior completely related to disturb the balance among divalent anion and cations (12,840 > 1530 + 460 ppm) which resulted in highly adsorbing of SO_4^{2-} on the calcite surface due to higher interaction in stern layer and better chemical interaction between positive surface charge (Ca^{2+}) and SO_4^{2-}. This phenomenon probably decreased the surface rock wettability alteration value in the presence of carboxylic groups and provided a critical condition to divalent cations, finally cations strongly stick to the calcite surface instead of oil components [14,21]. It is noteworthy to mentioned that, due to HCO_3^- low concentration (150 ppm) in sea water, the effect of HCO_3^- monovalent anion was neglected.

To quantify effects of the smart water solutions on the carbonated rock, the contact angle measurement was used. The effects of solutions were evaluated based on the net changes in the contact angle and after the wettability alteration in 168 h. A total of 11 solutions without the addition of any chemicals were prepared to check the effects of the excess amount of Ca^{2+}, Mg^{2+}, and SO_4^{2-} on the wettability modification. According to Table 4, all slices underwent a similar shift toward the strongly oil-wet condition. The high oil wetness of the carbonate rocks referred to the impact of the oil acidity. Some slices showed higher oil wetness in comparison with the rest of the slices which could be attributed to the high heterogeneity of the cross-sections.

Sea water was premised as the base water for analyzing the wettability alteration tests in the presence of different ion concentrations. In following sections, the wettability alterations were measured at an excess concentration of Ca^{2+}, Mg^{2+}, and SO_4^{2-}.

3.2.3. Effect of divalent cations on contact angle

Comparing net wettability changing by SW and DIW as a based smart water solution showed that the net wettability alteration was equal to 46° ± 2 versus 8° ± 0.4 after 168 h because of the existence of monovalent and divalent ions (Fig. 5a). It was assumed that the partial rock dissolution was occurred for DIW after 168 h, resulting in the low speed and poor wettability change [35,66].

Fig. 5b exhibits the different amounts of Ca^{2+} concentration in the sea water. It was found that an increase in Ca^{2+} concentration led to a more water-wet carbonate surface. In the earlier time (0–72 h) the pace of wettability alteration was slow (from 0° to 25°), however, among the 72 to 168 h, a drastic shift occurred in contact angle change (~65°). Confirming that four times excess amount Ca^{2+} had a great impact on the altering surface bar into positive. Furthermore, maintaining the rest of ions concentration, the Na^+ concentration in SW4Ca get decreased the contact compared to SW. Lower Na^+ ions concentration compared to SW into stern layer led to a performance better for Ca^{2+} ion through the double-layer expansion mechanism to desorb the carboxylic groups from rock and change the wettability alteration into more water-wet state [25,33].

Fig. 5c depicts the role of Mg^{2+} on the contact angle measurement. Results suggested the Mg^{2+} ion played a role of the acid removal element in the oil-wet surface and showed that the two times excess amount of Mg^{2+} led to a higher wettability alteration (~76° ± 2) which was corroborated zeta potential results. Based on the zeta potential results, four times excess amount of Mg^{2+} had better wettability alteration compared to SW2Mg, however, the amount of the wettability change in SW4Mg was descending. Excess amount of Mg^{2+} in SW4Mg, strongly disrupted the thermodynamic balance between divalent anion and cations which resulted in creating an extra positive charge on calcite surfaces and adsorbing SO_4^{2-} near the carboxylic groups. Moreover, decreasing the excessive Na^+ ions concentration effect on the behavior completely controlled the Ca^{2+} interaction with oil components in stern layer and could not be able to desorb the carboxylic groups efficiently from calcite rock surface. Results demonstrated that Mg^{2+} ions were capable to obliterate the strongly adsorbed carboxylate groups from the surface grain by changing the surface charge into positive and modify the wettability of rocks toward a higher water-wet state in optimum concentration (SW2Mg). Besides, decreasing the concentration of Na^+ in SW2Mg compared to SW had a great impact on the wettability modification and DLE mechanism dominated in this condition. Although, decreasing the excessive amount of Na^+ and gradually increasing Cl^- concentration in SW4Mg had a negative effect on the performance of Mg^{2+} and SO_4^{2-}, simultaneously. This behavior showed that the interaction of Ca^{2+} depended on the molecular size and ions activity. Ca^{2+} with higher reaction rate (higher atomic number and bigger electronic layer) but due to the molecular size compare to Mg^{2+} needed more effective time to enter the chemical interaction co-desorbed the carboxylic groups with SO_4^{2-}, close to calcite surface. In other words, excess amount of Ca^{2+} enhanced the positive charge of rock surface and assisted with SO_4^{2-} to release the crude oil droplet as a function of time. As well as, Fig. 5b and c demonstrated SW0Ca and SW0Mg, about four times higher concentration of Mg^{2+} in SW than Ca^{2+} concentration, had approximately an equal wettability alteration. Therefore, it could be understanding that in the absence of Ca^{2+}, SO_4^{2-} had an important role in activating a portion of Mg^{2+} ions in the solution (due to hydration bond) and co-desorbing the carboxylic groups from the rock surface. Other side, this behavior supported that Ca^{2+} ions had much higher chemical activity compared to Mg^{2+} ions even at quarter of Mg^{2+} ions concentration. It is noteworthy to be mentioned that, a portion of Mg^{2+} ions entered to the chemical reaction in the presence of SO_4^{2-} ions because of its higher concentration and became activated near the surface rock to desorb the surface-active agents present in the crude oil.

3.2.4. Effect of divalent anion on contact angle

Fig. 5d shows the impact of excess SO_4^{2-} ions concentration on the wettability alteration during 168 h. Increasing SO_4^{2-} ions concentration resulted in a more water-wet carbonate surface. However, wettability alteration for four times excess amount of SO_4^{2-} was lower than that of SW2S due to highly negative effect on the rock surface charge and disturbing the thermodynamic balance around the rock surface by Na^+ and Cl^- concentration decrease. The highest amount of wettability alteration was recorded at SW2S with a value of 107° ± 3. Dwindling the Cl^- concentration and controlling the Na^+ concentration created an elegant chance for SO_4^{2-} to access the rock surfaces. Based on this behavior, water film became thicker close to the surface due to the repulsive electrostatic forces between rock surface and the crude oil interface which resulted in much better alteration into water-wet state and desorb carboxylic groups. According to zeta potential measurements, SW2S shift decreased the negative value of surface bar and made a thermodynamic balance on the surface rock to a drastic change in the wettability alteration in the presence of Mg^{2+}, Ca^{2+}, and an appropriate concentration of monovalent ions [25]. In the case of the SW0S, the comparison of the net wettability changes after the treatment with and without SO_4^{2-} revealed that SO_4^{2-} was the most effective component in removing the acidic groups from the rock surfaces. Generally, multi ionic exchange was an outcome of the interaction among divalent cations, SO_4^{2-}, and carboxylic groups. Based on the results, the weakest wettability change occurred in the absence of SO_4^{2-} ions (7° ± 0.15) compared to divalent ions absence. This behavior confirmed that the

Table 4
The initial contact angle of cross-sections at different brine solutions.

Solutions	DIW	SW	SW0Ca	SW2Ca	SW4Ca	SW0S	SW2S	SW4S	SW0Mg	SW2Mg	SW4Mg
Initial CA	150°	145°	147°	140°	132°	139°	140°	147°	135°	126°	135°

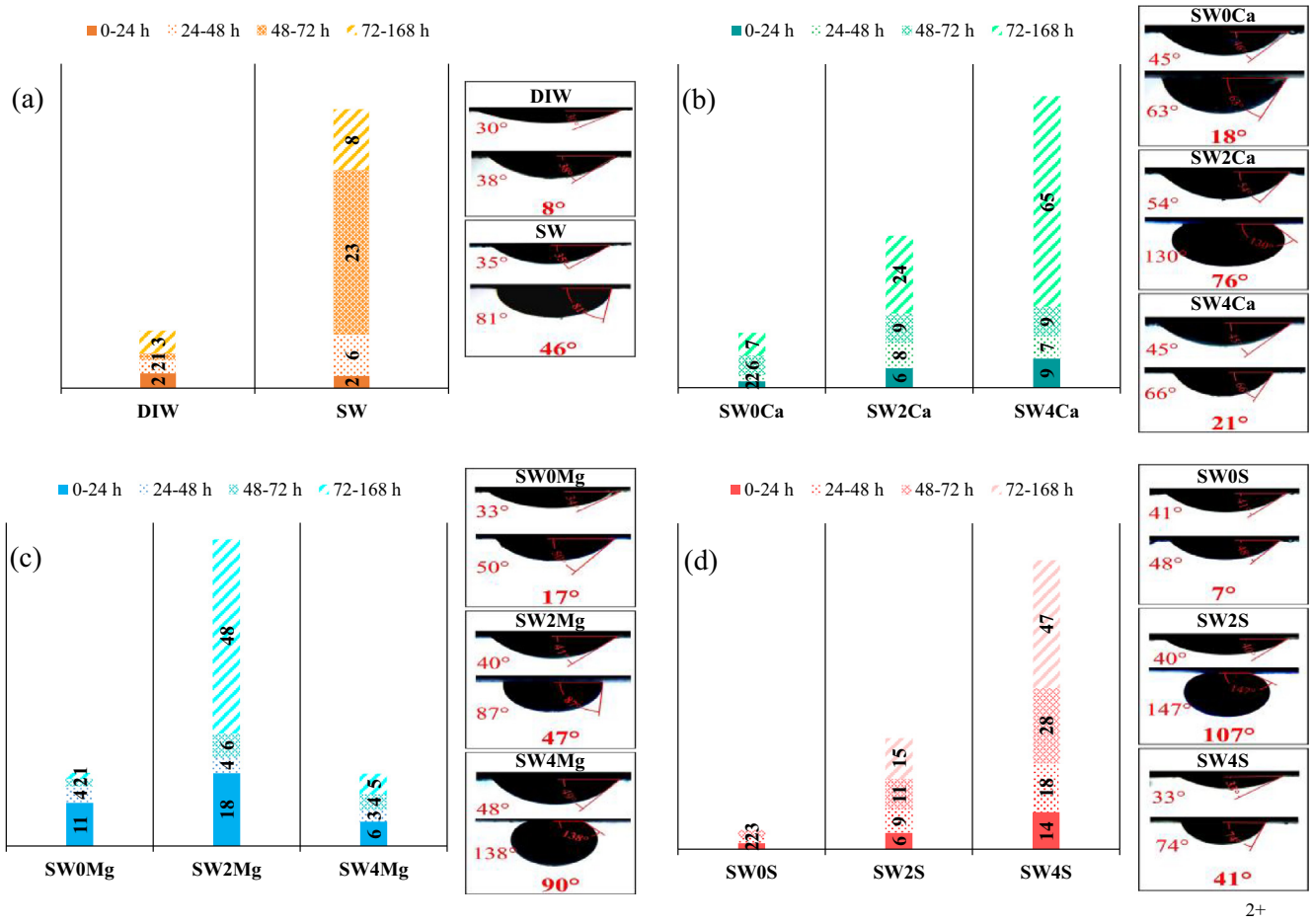

Fig. 5. a) Wettability alteration and oil droplet images for a) sea water and deionized water, b) excess Ca^{2+} solution, c) excess Mg^{2+} solution, d) excess SO_4^{2-} solution in the presence of salinity after 168 h at room temperature.

presence of SO_4^{2-} ions in the brine of calcite rocks as a catalyst to activate divalent cations [1].

According to the outcomes, Fig. 6 demonstrates the main mechanisms of individually divalent ions on the crude oil desorption from the rock surface. Fig. 7a to g illustrates the sea water and different ions concentration behavior (SW0S, SW2Mg, SW2S, SW4Ca, SW4Mg, and SW4S) based on zeta potential and contact angle tests. In this study, it was illustrated that an increase in the number of divalent ions depending on the ion's compatibility, zeta potential and appropriate ions concentration, which could lead to the effective wettability modification of the carbonate rock surfaces toward a more water-wet state even at room temperature. Indeed, the wettability alteration, a time-dependent process, was caused by the desorption of negatively-charged components within the crude oil. Potential determining ions

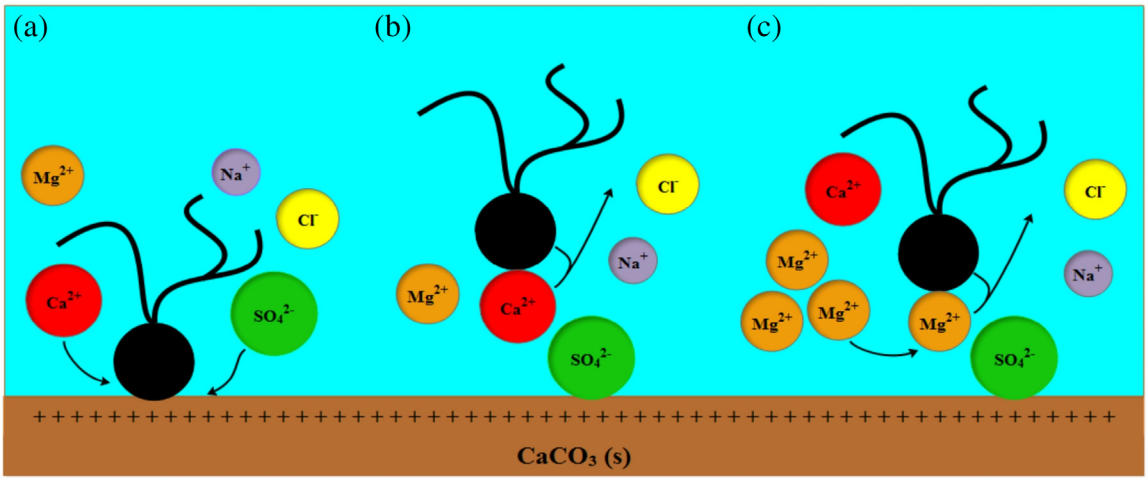

Fig. 6. Schematic of divalent ions individually performance in the presence of each other on wettability alteration in ambient condition.

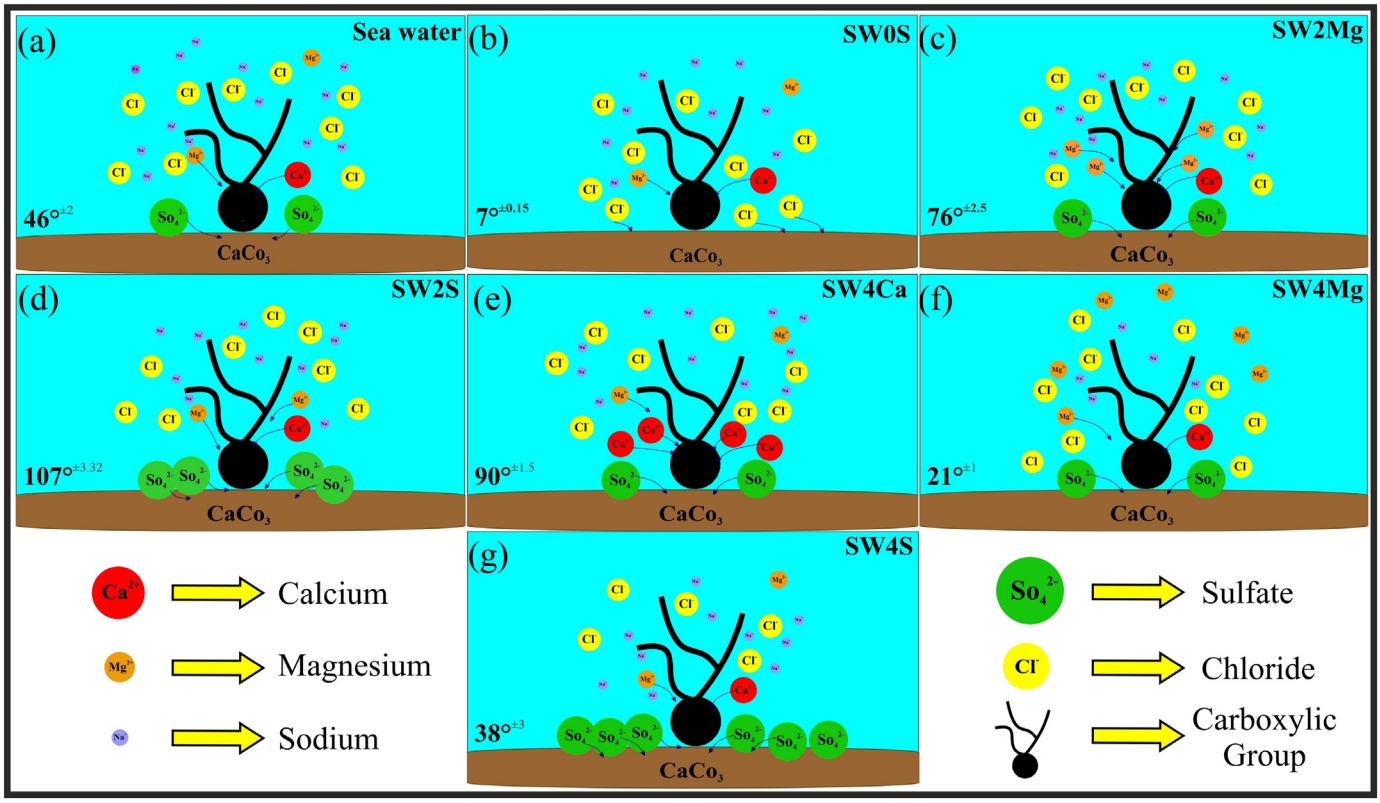

Fig. 7. Schematic of sea water and different divalent ions concentration effect according to zeta potential and contact angle results on crude oil desorption from the rock surface.

(Ca^{2+}, Mg^{2+}, and SO_4^{2-}) was the main reason of multicomponent exchange ions which was resulted in desorbed the carboxylic groups from the calcite rock in the presence of divalent cations (Mg^{2+} and Ca^{2+}) and replaced it with SO_4^{2-} [67,68]. The exclusion of Na^+ and Cl^- ions from the brine solutions improved the roles of the rest of the ions existing in the sea water especially for SW2S and SW4Ca. The presence of the divalent cations in the smart water after 168 h was vital for an effective wettability alteration process. A different type of smart water with a lower amount of Na^+ and Cl^- could perform better than SW due to the double layer expansion. However, the presence of monovalent ions in the vicinity of divalent ions was a crucial factor for a better wettability modification. It was well understood that Ca^{2+} and SO_4^{2-} were more effective than Mg^{2+} and monovalent ions. Besides, immersing the calcite rock slices in the brine solutions, it was observed that the wettability change was very much fortified by adding the excess SO_4^{2-} concentration. However, the speed of the wettability alteration in excess Mg^{2+} ion was higher than the SO_4^{2-} and Ca^{2+}. It could be noteworthy to mention that the interplay between Ca^{2+}, and SO_4^{2-} was the key factor for removing acidic components from the oil-wet surfaces at the room temperature. The outcomes from wettability alteration tests for smart water solutions supported that the sea water with two times excess SO_4^{2-} concentration was the most effective and practical solution.

3.3. IFT measurement

The interfacial tension values between the oil and smart waters are represented in Fig. 8. According to the previous studies, the IFT between the high saline water and oil was high due to the existence of various ions with high concentration, which resulted in decreasing fluid-fluid interaction and increasing bypassed oil [2]. Refer to researchers' suggestion to use selective ions for improving IFT reduction, it was essential to measure this parameter in order to detect the appropriate smart water solutions with a preferable impact. Keeping the constant salinity concentration in all smart waters at 40,572 ppm, the kind of ion altered in the sea water was the only changeable element for interfacial tension measurements. IFT value for DIW and SW as a based comparative fluid were 22.1 and 19.3 dyne/cm, respectively. Comparing the IFT results for smart waters revealed that decreasing the number of divalent ions caused in IFT increasing, especially in the case of Mg^{2+}. This behavior was taken from Mendeleev's periodic table that Mg^{2+} has smaller atomic radius compared to Ca^{2+} which is resulted in higher charge density. Hence, Mg^{2+} had effective chemical interaction with surface active agent from crude oil (resin and asphaltene) [65]. According to the SARA analysis of the oil phase, it was noticed that the oil sample was mainly composed of saturating and aromatic components. Enhancing the concentration of $MgCl_2$ and $CaCl_2$ in aqueous solution motivated resin and asphaltene molecules to transfer into the interface, while monovalent ions such as sodium chloride did not intend to transfer the resin and asphaltene contents [31]. On the other hand, the addition of SO_4^{2-} had a lower effect on the IFT value compared to divalent cations. SO_4^{2-} preferred to participate in chemical interaction with rock surface (rock/fluid) due to properties. To magnify the positive impact of Mg^{2+} and Ca^{2+} on the IFT reduction it was necessary to reduce the amount of Na^+ and Cl^-. Adding different salts to the system could change the natural surfactant distribution (including asphaltene and resin) at the fluid/fluid interface along with electrostatic forces effects and consequently, the IFT values changed. However, the IFT reduction for different excess divalent ions in the presence of salinity was not impressive compared to chemicals such as surfactants [6,69].

3.4. Carbonated coated micromodel flooding tests

To justify the recovery factor results and investigate the pore-scale mechanisms, flooding tests for deionized water as a conventional waterflooding process, sea water, and selected smart waters (SW2Mg, SW4Ca, and SW2S) based on the compatibility, zeta potential, contact

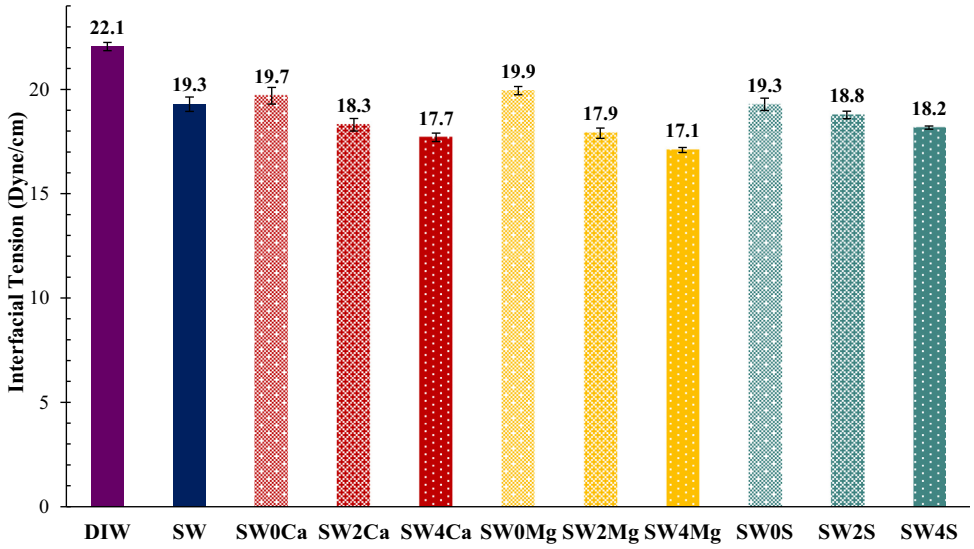

Fig. 8. IFT value between the oil and different smart water solutions.

angle and IFT results were conducted. According to Fig. 9 to show the oil recovery results, breakthrough started at earlier time after 0.22 pore volume injection in all waterflooding injections. Because of the high mobility ratio, the water fingering process happened in DIW flooding caused an acceleration in the breakthrough time, the mobility ratio increased and finally the water channeling phenomenon occurred. After breakthrough point, the oil recovery value did not significantly change and it was achieved as 26.2% by DIW flooding. Moreover, after 2 pore volume injections, high amount of the residual oil around the surface grain was observed.

The amount of recovery factor for SW, SW2Mg, SW4Ca, and SW4S was 30.4, 32.9, 34, and 38%, respectively. The similar viscosity of sea water and smart water solution with DIW, homogenous pattern, and water channeling phenomenon occurred, all three reasons caused to obtain the same breakthrough after 0.22 pore volume like DIW flooding, resulting in not considerably change in the oil recovery value after the breakthrough time. However, the recovery factor for the value smart waters was higher than that of DIW flooding due to the wettability alteration, higher IFT reduction, emulsification mechanism and also lower discontinuity. It is essential to mention that, the difference in oil recovery numbers are low meaning that the differences plotted in the Fig. 9 between the cases are significant and hence are caused by differences in the water compositions used.

3.4.1. Effects of salts on residual oil in smart waterflooding

Having the higher final oil recovery for SW2S than that of the other flooding agents with the same breakthrough in Fig. 9, microscopically comparing the flooding patterns and residual oil in Fig. 10a, b showed the less amount of residual oil around the carbonated coated grains for the case of SW2S flooding. This phenomenon resulted from the effect of the injected fluid in the IFT reduction between the fluid/fluid interaction and wettability alteration rock/fluid interaction, presenting the below results in aforementioned sections:

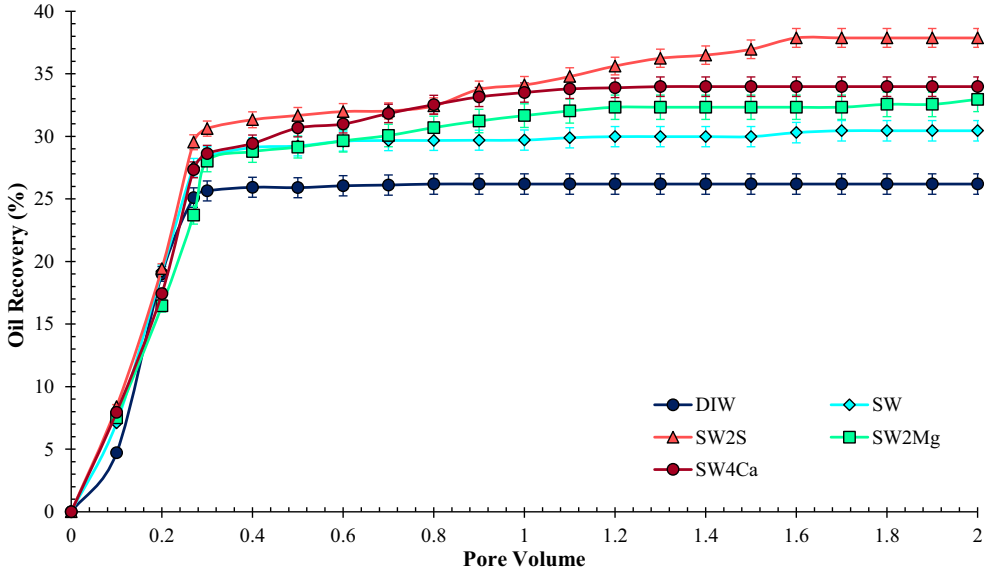

Fig. 9. Oil recovery factor after 2 PV injection of deionized water, sea water and smart water solutions in glass coated micromodel.

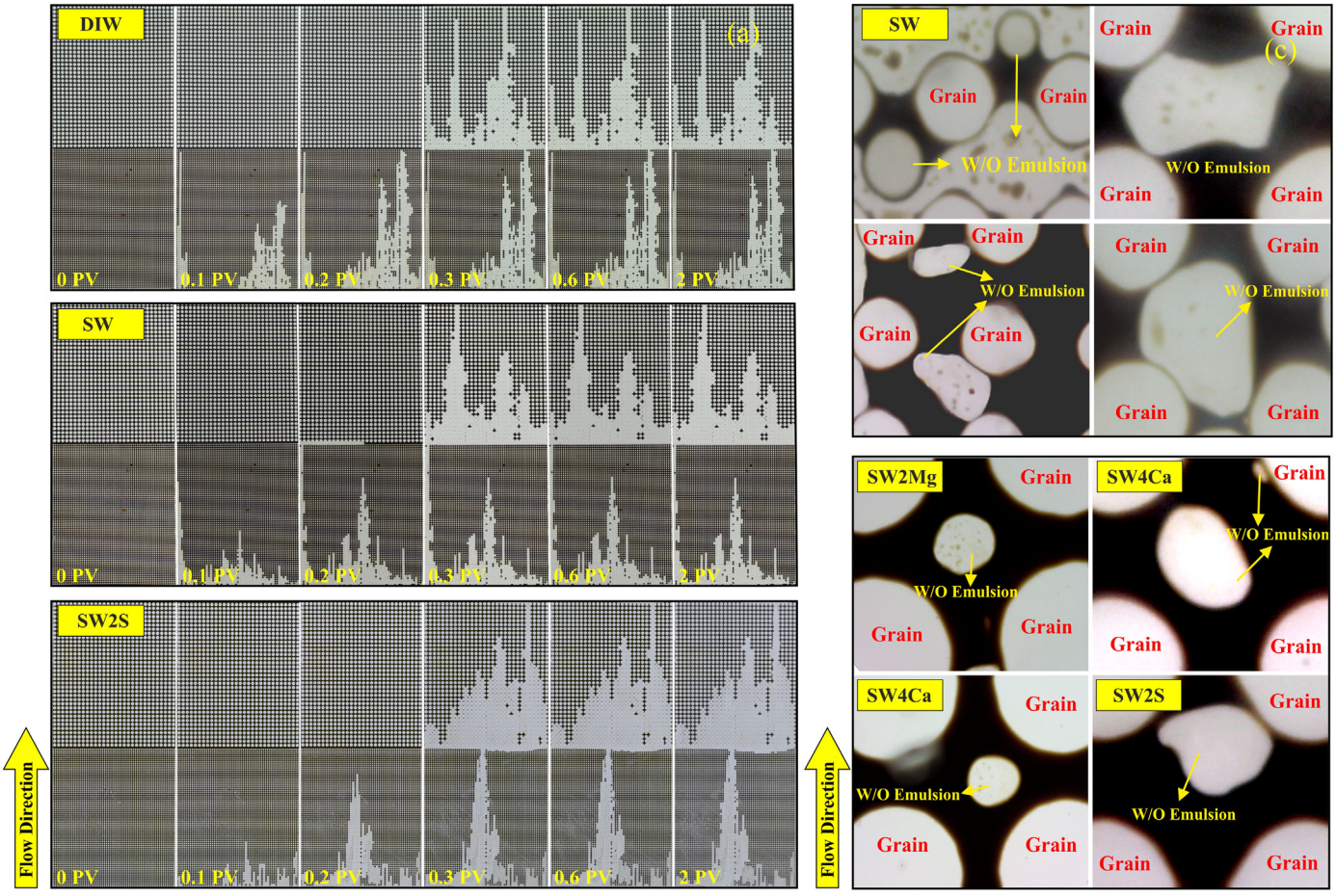
DIW
SW
SW2S
0 PV
0.1 PV
0.2 PV
0.3 PV
0.6 PV
2 PV
(a)
Flow Direction
SW
Grain
W/O Emulsion
(c)
SW2Mg
SW4Ca
SW2S

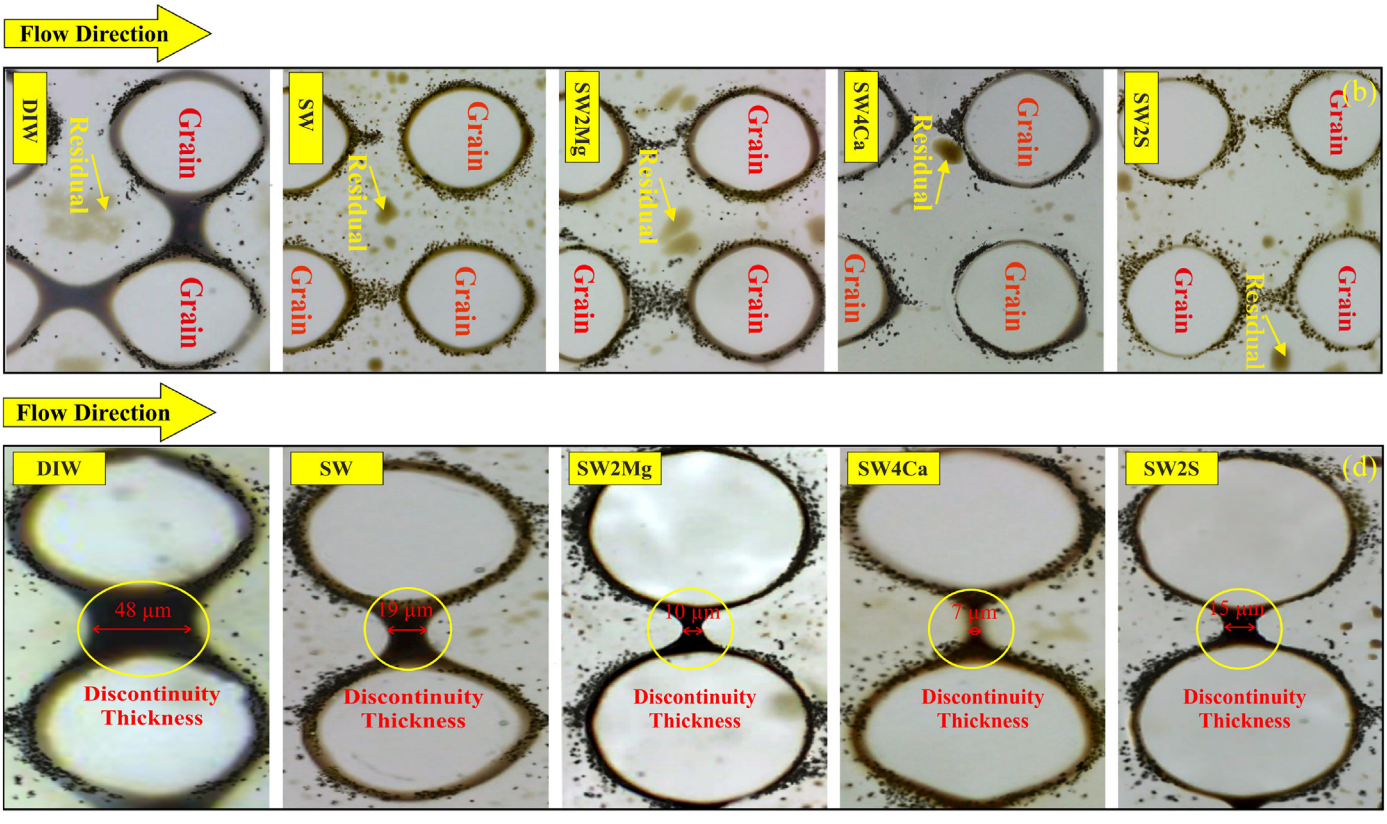
Flow Direction
DIW
SW
SW2Mg
SW4Ca
SW2S
Grain
Residual
(b)
Flow Direction
48 µm
19 µm
10 µm
7 µm
15 µm
Discontinuity Thickness
(d)

Zeta potential : SW4S<SW2S<SW0Mg<SW0Ca<SW<SW2Ca<SW0S <SW2Ca<SW4Ca<SW4Mg

Wettability alteration : SW0S<SW0Ca<SW0Mg<SW4Mg<SW4S<SW <SW2Ca<SW2Mg<SW4Ca<SW2S

IFT Reduction : SW0Mg<SW0Ca<SW0S<SW<SW2S<SW2Ca ~ SW4S<SW2Mg ~ SW4Ca<SW4Mg

3.4.2. Emulsification mechanism at pore-scale

Fig. 10c shows the water trapping happened among the oil layers for DIW, SW and SW4S solutions, defined as water in oil emulsion at the pore-scale. The existence of surface-active materials like Mg^{2+}, Ca^{2+}, resin, and asphaltene as the third component in an emulsification process resulted in the IFT reduction between two phases and could stabilize and increase the number of dispersed droplets. The water droplets were dragged into the oil pool in the vicinity of the interface between the two phases. Moreover, in constant rate better, smaller, and more stable water in oil droplets occurred in higher capillary number areas (bigger pore throat). Other side, the impact of emulsion droplet size distribution was expected to dominate the oil recovery flow mechanism [70]. The water in oil emulsion coming from the presence of ions facilitated the flow of displaced phase in the invasion zone and improved the final swept efficiency during 2 PV injections. No droplets occurred in deionized water in both high and low permeable zone due to the absence of ions, the emulsion droplet size in SW was slightly bigger than that of smart water which agreed with the Maaref et al. results about the effect of IFT and optimum divalent ions at the fluid/fluid interface on the emulsion size droplet and the ultimate recovery [50].

3.4.3. Fingering mechanism and discontinuity phenomenon at pore-scale

Results from Fig. 10d revealed a direct impact of the pore throat size on the discontinuity thickness. The number of interruptions and fingering intensities in smaller pore throat areas was higher than the bigger pore throat. This effect interrupted the displacing fluid, which resulted in decreasing the final oil recovery. The discontinuity in the matrix resulted from the fingering problem during the flooding process where was lower for the aqueous solutions in the high permeable areas due to the lower capillary number. The non-wet phase preferred to move through the lower capillary pressure-pore throats, a better flow distribution was yielded to increase the fluid flow duration into the larger pore throats areas. Consequently, it provided enough time for the aqueous solutions to be in contact with the oil phase to affect the IFT reduction value and wettability alteration. Therefore, the number of discontinuities decreased in the high permeable zone. Generally speaking, the fingering mechanism distribution had a significant impact on raising the number of discontinuities in the porous media with different pore throat sizes. Besides, the thickness of residual oil among most of the grains in the presence of salinity became thinner after 2 PV injections due to the effective interaction between the salinity, powder grain, and crude oil.

4. Conclusion

This study was outlined the symbiotic effects of different ions concentration (SO_4^{2-}, Mg^{2+}, and Ca^{2+}) as smart water solutions on carbonated reservoir mechanisms including compatibility, surface charge by zeta potential, wettability alteration, and IFT reduction at macro and micro scale. A coated carbonated micromodel was developed to evaluate the effects of selected smart water on the ultimate oil recovery and the pore-scale mechanisms. According to the experimental analyses, the wettability alteration was the most effective mechanism. Next, three smart water solutions, SW2S, SW4Ca, and SW2Mg alongside DIW and SW were selected for the micromodel flooding tests. It was found that the SW2S had the best performance through the flooding procedure compared with other aqueous solution by checking residual oil, water in oil emulsifications, and number and diameters of discontinuity. The essential findings were summarized as follows:

- All of the saline waters were compatible with smart water solutions and no precipitation was observed at 80 °C. The outcomes represented that the order of the addition of different salts into deionized water was important avoiding any precipitation. However, four times excess amount of SO_4^{2-} slightly precipitated in the presence of formation brine at 80 °C.
- The influence of divalent ions on surface charge was investigated by zeta potential experiments. Results depicted as much as the excess amount of divalent cations and anions high, the process of changing the surface charge into positive and negative values took more intensive. The zeta potential values comparison outlined as below:

SW4S<SW2S<SW0Mg<SW0Ca<SW<SW2Ca<SW0S<SW2Ca<SW4Ca<SW4Mg

- Higher potential in the wettability alteration was achieved by using two times excess amount of SO_4^{2-} in the sea water after 168 h. Results represented that optimum divalent and monovalent ions concentration could be more effective to desorb the carboxylic group from the rock surface. The effect divalent ions concentration in the brines on altering wetting state compared as below:

SW0S<SW0Ca<SW0Mg<SW4Mg<SW4S<SW<SW2Ca<SW2Mg<SW4Ca<SW2S

- IFT results revealed that using the saline waters reduced the IFT for all cases and excess amount of divalent cations were found to have a better impact on IFT reduction. However, no considerable relation among fluid/fluid interaction and smart water solution was observed. The activity of brine solutions in IFT reduction were given below:

SW0Mg<SW0Ca<SW0S<SW<SW2S<SW2Ca ~ SW4S<SW2Mg ~ SW4Ca<SW4Mg

- Based on experimental results, SW2S, SW2Mg, and SW4Ca were selected as the suitable smart water solutions for smart waterflooding in coated carbonated micromodel. SW2S produced more oil compared to DIW, sea water and other smart waters, attributed to the lower residual oil and better performance on microscopic mechanisms. The final ultimate recovery was in the following order:

DIW<SW<SW2Mg<SW4Ca<SW2S

Fig. 10. a) Distribution of the aqueous solutions (DIW, SW, and SW2S) and crude oil in micromodel during six different time steps of 0, 0.1, 0.2, 0.3, 0.6, and 2 PV, b) effect of salinity on the residual oil amount around grain after 2 PV injection in glass micromodel, c) evidence of water in oil emulsification in smart waterflooding, d) thickness of discontinuity in DIW, SW, SW2Mg, SW4Ca, and SW2S after 2 PV injection in coated micromodel (all tests at room temperature).

CRediT authorship contribution statement

A. Maghsoudian: Formal analysis Data curation, Writing - original draft, Conceptualization. **A. Esfandiarian:** Data curation, Investigation. **S. Kord:** Conceptualization, Methodology, Supervision, Writing - review & editing. **Y. Tamsilian:** Conceptualization, Methodology, Supervision, Writing - review & editing. **B. Soltani Soulgani:** Writing - review & editing.

Declaration of competing interest

The authors declare that they have no known competing financial interests or personal relationships that could have appeared to influence the work reported in "Direct insights into the micro and macro scale mechanisms of symbiotic effect of SO_4^{2-}, Mg^{2+}, and Ca^{2+} ions concentration for smart waterflooding in the carbonated coated micromodel system".

References

[1] E.W. Al-Shalabi, K. Sepehrnoori, A comprehensive review of low salinity/engineered water injections and their applications in sandstone and carbonate rocks, J. Pet. Sci. Eng. 139 (2016) 137–161, https://doi.org/10.1016/j.petrol.2015.11.027.

[2] M. Derkani, A. Fletcher, W. Abdallah, B. Sauerer, J. Anderson, Z. Zhang, Low salinity waterflooding in carbonate reservoirs: review of interfacial mechanisms, Colloids Interfaces 2 (2018) 20, https://doi.org/10.3390/colloids2020020.

[3] A.A. Yousef, S.H. Al-Saleh, A. Al-Kaabi, M.S. Al-Jawfi, Laboratory investigation of the impact of injection-water salinity and ionic content on oil recovery from carbonate reservoirs, SPE Reserv. Eval. Eng. 14 (2011) 578–593.

[4] T. Austad, Water based EOR in carbonates and sandstones: new chemical understanding of the EOR-potential using " smart water", Enhanc. Oil Recover. F. Cases 2013, pp. 301–332.

[5] S. Strand, T. Puntervold, T. Austad, Water based EOR from clastic oil reservoirs by wettability alteration: a review of chemical aspects, J. Pet. Sci. Eng. 146 (2016) 1079–1091.

[6] J. Hao, S. Mohammadkhani, H. Shahverdi, M.N. Esfahany, A. Shapiro, Mechanisms of smart waterflooding in carbonate oil reservoirs-a review, J. Pet. Sci. Eng. 179 (2019) 276–291.

[7] F. Liu, M. Wang, Review of low salinity waterflooding mechanisms: wettability alteration and its impact on oil recovery, Fuel 267 (2020), 117112. .

[8] T. Austad, A. Rezaeidoust, T. Puntervold, Chemical mechanism of low salinity water flooding in sandstone reservoirs, SPE Improv. Oil Recover. Symp, 2010https://doi.org/10.2118/129767-MS.

[9] H. Mahani, S. Berg, D. Ilic, W.-B. Bartels, V. Joekar-Niasar, Kinetics of the low salinity waterflooding effect studied in a model system, SPE Enhanc. Oil Recover. Conf, Society of Petroleum Engineers, 2013.

[10] P.C. Myint, A. Firoozabadi, Thin liquid films in improved oil recovery from low-salinity brine, Curr. Opin. Colloid Interface Sci. 20 (2015) 105–114, https://doi.org/10.1016/j.cocis.2015.03.002.

[11] P.L. McGuire, J.R. Chatham, F.K. Paskvan, D.M. Sommer, F.H. Carini, Low Salinity Oil Recovery: An Exciting New EOR Opportunity for Alaska's North Slope, SPE West. Reg. Meet, 2005 1–15, https://doi.org/10.2118/93903-MS.

[12] M.B. Alotaibi, R. Azmy, H.A. Nasr-El-Din, Wettability challenges in carbonate reservoirs, SPE Improv. Oil Recover. Symp, Society of Petroleum Engineers, 2010.

[13] J. Abubacker, H. Al-Attar, A. Zekri, M. Khalifi, E. Louiseh, Selecting a potential smart water for EOR implementation in Asab oil field, J. Pet. Explor. Prod. Technol. 7 (2017) 1133–1147.

[14] M.H. Derkani, A.J. Fletcher, M. Fedorov, W. Abdallah, B. Sauerer, J. Anderson, Z.J. Zhang, Mechanisms of surface charge modification of carbonates in aqueous electrolyte solutions, Colloids Interfaces 3 (2019) 62.

[15] G.Q. Tang, N.R. Morrow, Influence of brine composition and fines migration on crude oil/brine/rock interactions and oil recovery, J. Pet. Sci. Eng. 24 (1999) 99–111, https://doi.org/10.1016/S0920-4105(99)00034-0.

[16] M.J. Barnaji, P. Pourafshary, M.R. Rasaie, Visual investigation of the effects of clay minerals on enhancement of oil recovery by low salinity water flooding, Fuel 184 (2016) 826–835.

[17] P. Zhang, T. Austad, Wettability and oil recovery from carbonates: effects of temperature and potential determining ions, Colloids Surf. A Physicochem. Eng. Asp. 279 (2006) 179–187, https://doi.org/10.1016/j.colsurfa.2006.01.009.

[18] D.J. Ligthelm, J. Gronsveld, J. Hofman, N. Brussee, F. Marcelis, H. van der Linde, Novel waterflooding strategy by manipulation of injection brine composition, Eur. Conf. Exhib. (2009) 1–22, https://doi.org/10.2118/119835-MS.

[19] S.Y. Lee, K.J. Webb, I.R. Collins, A. Lager, S.M. Clarke, M. O'Sullivan, A.F. Routh, Low salinity oil recovery–increasing understanding of the underlying mechanisms of double layer expansion, IOR 2011-16th Eur. Symp. Improv. Oil Recover, 2011.

[20] R.A. Nasralla, H.A. Nasr-El-Din, Double-layer expansion: is it a primary mechanism of improved oil recovery by low-salinity waterflooding? SPE Reserv. Eval. Eng. 17 (2014) 49–59.

[21] P. Ahmadi, H. Asaadian, A. Khadivi, S. Kord, A new approach for determination of carbonate rock electrostatic double layer variation towards wettability alteration, J. Mol. Liq. 275 (2019) 682–698.

[22] P. Zhang, M.T. Tweheyo, T. Austad, Wettability alteration and improved oil recovery in chalk: the effect of calcium in the presence of sulfate, Energy Fuel 20 (2006) 2056–2062.

[23] S.J. Fathi, T. Austad, S. Strand, "Smart water" as a wettability modifier in chalk: the effect of salinity and ionic composition, Energy Fuel 24 (2010) 2514–2519.

[24] W. Abdallah, A. Gmira, Wettability assessment and surface compositional analysis of aged calcite treated with dynamic water, Energy Fuel 28 (2014) 1652–1663, https://doi.org/10.1021/ef401908w.

[25] M. Shirazi, J. Farzaneh, S. Kord, Y. Tamsilian, Smart water spontaneous imbibition into oil-wet carbonate reservoir cores: symbiotic and individual behavior of potential determining ions, J. Mol. Liq. 299 (2020), 112102. .

[26] S. Strand, E.J. Høgnesen, T. Austad, Wettability alteration of carbonates—effects of potential determining ions (Ca2+ and SO42−) and temperature, Colloids Surf. A Physicochem. Eng. Asp. 275 (2006) 1–10.

[27] W.-B. Bartels, H. Mahani, S. Berg, S.M. Hassanizadeh, Literature review of low salinity waterflooding from a length and time scale perspective, Fuel 236 (2019) 338–353.

[28] B. Honarvar, A. Rahimi, M. Safari, S. Khajehahmadi, M. Karimi, Smart water effects on a crude oil-brine-carbonate rock (CBR) system: further suggestions on mechanisms and conditions, J. Mol. Liq. 299 (2020), 112173. .

[29] S.J. Fathi, T. Austad, S. Strand, Water Based EOR by "Smart Water": Optimal Ionic Composition for Enhanced Oil Recovery in Carbonates, 2011 1–17.

[30] E.J. Hoegnesen, EOR in Fractured Oil-wet Chalk. Spontaneous Imbibition of Water by Wettability Alteration, (PhD thesis) University of Stavanger, 2005.

[31] O. Karoussi, A.A. Hamouda, Imbibition of sulfate and magnesium ions into carbonate rocks at elevated temperatures and their influence on wettability alteration and oil recovery, Energy Fuel 21 (2007) 2138–2146, https://doi.org/10.1021/ef0605246.

[32] S.F. Shariatpanahi, P. Hopkins, H. Aksulu, S. Strand, T. Puntervold, T. Austad, Water based EOR by wettability alteration in dolomite, Energy Fuel 30 (2016) 180–187, https://doi.org/10.1021/acs.energyfuels.5b02239.

[33] S. Prabhakar, R. Melnik, Wettability alteration of calcite oil wells: influence of smart water ions, Sci. Rep. 7 (2017) 1–9.

[34] M. Lashkarbolooki, M. Riazi, F. Hajibagheri, S. Ayatollahi, Low salinity injection into asphaltenic-carbonate oil reservoir, mechanistical study, J. Mol. Liq. 216 (2016) 377–386, https://doi.org/10.1016/j.molliq.2016.01.051.

[35] A. Kakati, J.S. Sangwai, Effect of monovalent and divalent salts on the interfacial tension of pure hydrocarbonbrine systems relevant for low salinity water flooding, J. Pet. Sci. Eng. (2017)https://doi.org/10.1016/j.petrol.2017.08.017.

[36] S. Mohammadi, S. Kord, J. Moghadasi, The hybrid impact of modified low salinity water and anionic surfactant on oil expulsion from carbonate rocks: a dynamic approach, J. Mol. Liq. 281 (2019) 352–364, https://doi.org/10.1016/j.molliq.2019.02.092.

[37] A. Hiorth, L.M. Cathles, M.V. Madland, The impact of pore water chemistry on carbonate surface charge and oil wettability, Transp. Porous Media 85 (2010) 1–21, https://doi.org/10.1007/s11242-010-9543-6.

[38] E.W. Al Shalabi, K. Sepehrnoori, M. Delshad, Does the double layer expansion mechanism contribute to the LSWI effect on hydrocarbon recovery from carbonate rocks? SPE Reserv. Charact. Simul. Conf. Exhib, Society of Petroleum Engineers, 2013.

[39] M. Karimi, R.S. Al-Maamari, S. Ayatollahi, N. Mehranbod, Mechanistic study of wettability alteration of oil-wet calcite: the effect of magnesium ions in the presence and absence of cationic surfactant, Colloids Surf. A Physicochem. Eng. Asp. 482 (2015) 403–415, https://doi.org/10.1016/j.colsurfa.2015.07.001.

[40] T. Austad, S. Strand, T. Puntervold, Is wettability alteration of carbonates by seawater caused by rock dissolution, Pap. SCA2009-43 Present. Int. Symp. Soc. Core Anal. Held Noordwijk, Netherlands Sept., 2009, pp. 27–30.

[41] H. Al-Hashim, A. Kasha, W. Abdallah, B. Sauerer, Impact of modified seawater on zeta potential and morphology of calcite and dolomite aged with stearic acid, Energy Fuel 32 (2018) 1644–1656.

[42] D. Al Mahrouqi, J. Vinogradov, M.D. Jackson, Zeta potential of artificial and natural calcite in aqueous solution, Adv. Colloid Interf. Sci. 240 (2017) 60–76.

[43] Z. Yi, H.K. Sarma, Improving waterflood recovery efficiency in carbonate reservoirs through salinity variations and ionic exchanges: a promising low-cost "smart-waterflood" approach, Abu Dhabi Int. Pet. Conf. Exhib, Society of Petroleum Engineers, 2012.

[44] S. Mohammadi, S. Kord, J. Moghadasi, An experimental investigation into the spontaneous imbibition of surfactant assisted low salinity water in carbonate rocks, Fuel 243 (2019) 142–154, https://doi.org/10.1016/j.fuel.2019.01.074.

[45] A. Kakati, G. Kumar, J.S. Sangwai, Oil recovery efficiency and mechanism of low salinity-enhanced oil recovery for light crude oil with a low acid number, ACS Omega 5 (3) (2020) 1506–1518.

[46] S. Ayirala, A. Alghamdi, A. Gmira, D.K. Cha, M.A. Alsaud, A. Yousef, Linking pore scale mechanisms with macroscopic to core scale effects in controlled ionic composition low salinity waterflooding processes, Fuel 264 (2020), 116798. .

[47] A. Emadi, M. Sohrabi, Visual investigation of oil recovery by low salinity water injection: Formation of water micro-dispersions and wettability alteration, SPE Annu. Tech. Conf. Exhib, Society of Petroleum Engineers, 2013.

[48] A. Emadi, M. Sohrabi, Visual investigation of low salinity waterflooding, Int. Symp. Soc. Core Anal. Aberdeen, Scotland, UK 2012, pp. 27–30.

[49] T. Amirian, M. Haghighi, P. Mostaghimi, Pore scale visualization of low salinity water flooding as an enhanced oil recovery method, Energy Fuel 31 (2017) 13133–13143.

[50] S. Maaref, S. Ayatollahi, N. Rezaei, M. Masihi, The Effect of Dispersed Phase Salinity on Water-in-oil Emulsion Flow Performance: A Micromodel Study the Effect of Dispersed Phase Salinity on Water-in-oil Emulsion Flow Performance: A Micromodel

Study Abstract in this Work, the Effect of Brine Salinity on Water-in-oil Emulsion Flow Performance in a Porous, 2017https://doi.org/10.1021/acs.iecr.7b00432.
[51] P. Rostami, M.F. Mehraban, M. Sharifi, M. Dejam, S. Ayatollahi, Effect of water salinity on oil/brine interfacial behaviour during low salinity waterflooding: a mechanistic study, Petroleum 5 (2019) 367–374.
[52] H. Ding, Y. Wang, A. Shapoval, Y. Zhao, S. Rahman, Macro-and microscopic studies of "smart water" flooding in carbonate rocks: an image-based wettability examination, Energy Fuel 33 (2019) 6961–6970.
[53] M. Mohammadi, H. Mahani, Direct insights into the pore-scale mechanism of low-salinity waterflooding in carbonates using a novel calcite microfluidic chip, Fuel 260 (2020), 116374. .
[54] D. Vazquez, G.A. Mansoori, Identification and measurement of petroleum precipitates, J. Pet. Sci. Eng. 26 (2000) 49–55.
[55] M.H. Sedaghat, M.H. Ghazanfari, M. Masihi, D. Rashtchian, Experimental and numerical investigation of polymer flooding in fractured heavy oil five-spot systems, J. Pet. Sci. Eng. 108 (2013) 370–382, https://doi.org/10.1016/j.petrol.2013.07.001.
[56] O. Mohammadzadeh, M.H. Sedaghat, S. Kord, S. Zendehboudi, J.P. Giesy, Pore-level visual analysis of heavy oil recovery using chemical-assisted waterflooding process – use of a new chemical agent, Fuel 239 (2019) 202–218, https://doi.org/10.1016/j.fuel.2018.10.104.
[57] Khalafi, A. Hashemi, M. Zallaghi, R. Kharrat, An experimental investigation of nanoparticles assisted surfactant flooding for improving oil recovery in a micromodel system, J. Pet. Environ. Biotechnol. 9 (2018).
[58] D.W. Green, G.P. Willhite, Enhanced Oil Recovery, Society of Petroleum Engineers, 1998https://store.spe.org/Enhanced-Oil-Recovery–P21.aspx.
[59] W. Song, A.R. Kovscek, Functionalization of micromodels with kaolinite for investigation of low salinity oil-recovery processes, Lab Chip 15 (2015) 3314–3325.
[60] A. Kasha, H. Al-Hashim, W. Abdallah, R. Taherian, B. Sauerer, Effect of Ca2+, Mg2+ and SO42− ions on the zeta potential of calcite and dolomite particles aged with stearic acid, Colloids Surf. A Physicochem. Eng. Asp. 482 (2015) 290–299.
[61] W.G. Anderson, Wettability literature survey-part 1: rock/oil/brine interactions and the effects of core handling on wettability, J. Pet. Technol. 38 (1986) 1125–1144, https://doi.org/10.2118/13932-PA.
[62] P. Abbasi, S. Abbasi, J. Moghadasi, Experimental investigation of mixed-salt precipitation during smart water injection in the carbonate formation, J. Mol. Liq. 299 (2020), 112131. .
[63] S. Kumar, P. Panigrahi, R.K. Saw, A. Mandal, Interfacial interaction of cationic surfactants and its effect on wettability alteration of oil-wet carbonate rock, Energy Fuel 30 (2016) 2846–2857.
[64] N.S. Labidi, Studies of the mechanism of polyvinyl alcohol adsorption on the calcite/water interface in the presence of sodium oleate, J. Miner. Mater. Charact. Eng. 7 (2008) 147.
[65] Y. Kazemzadeh, I. Ismail, H. Rezvani, M. Sharifi, M. Riazi, Experimental investigation of stability of water in oil emulsions at reservoir conditions: effect of ion type, ion concentration, and system pressure, Fuel 243 (2019) 15–27.
[66] P. Vledder, I.E. Gonzalez, J.C. Carrera Fonseca, T. Wells, D.J. Ligthelm, Low salinity water flooding: proof of wettability alteration on a field wide scale, SPE Improv. Oil Recover. Symp, Society of Petroleum Engineers, 2010.
[67] A. Kilybay, B. Ghosh, N. Chacko Thomas, A review on the progress of ion-engineered water flooding, J. Pet. Eng. 2017 (2017) 1–9, https://doi.org/10.1155/2017/7171957.
[68] H. Ding, S.R. Rahman, Investigation of the impact of potential determining ions from surface complexation modeling, Energy Fuel 32 (2018) 9314–9321.
[69] M. Shirazi, S. Kord, Y. Tamsilian, Novel smart water-based titania nanofluid for enhanced oil recovery, J. Mol. Liq. 296 (2019), 112064. .
[70] G.A. Pietrangeli, L. Quintero, T.A. Jones, Q. Darugar, Treatment of water in heavy crude oil emulsions with innovative microemulsion fluids, SPE Heavy Extra Heavy Oil Conf. Lat. Am, Society of Petroleum Engineers, 2014.